Sgo1 establishes the centromeric cohesion protection mechanism in G2 before subsequent Bub1-dependent recruitment in mitosis

David Perera and Stephen S. Taylor*

Faculty of Life Sciences, University of Manchester, Michael Smith Building, Oxford Road, Manchester M13 9PT, UK

*Author for correspondence (stephen.taylor@manchester.ac.uk)

Accepted 17 December 2009
Journal of Cell Science 123, 653-659

doi:10.1242/jcs.059501

Summary

Bub1 was one of the first protein kinases identified as a component of the spindle-assembly checkpoint, a surveillance mechanism that delays anaphase onset until all chromosomes are stably attached to spindle microtubules. Whereas the kinase activity of Bub1 is not required for checkpoint function in yeast, its requirement in mammalian cells is still unclear. Using a complementation assay with bona fide *BUB1*-null mouse embryonic fibroblasts, we show that the kinase activity of Bub1 is not required for checkpoint function or chromosome alignment. Its activity is, however, required for centromeric localisation of Sgo1, a known protector of centromeric cohesion. Despite the absence of Sgo1 from mitotic centromeres in cells devoid of Bub1 activity, centromeric cohesion is still maintained until anaphase. An explanation for this comes from observations showing that Sgo1 is first recruited to centromeric heterochromatin in G2, but then becomes diffusely localised throughout the nucleus in early prophase, before returning to centromeres later in prophase. Importantly, whereas centromeric localisation of Sgo1 in prophase is dependent on the kinase activity of Bub1, its recruitment to centromeric heterochromatin in G2 is not. Rather, the localisation of Sgo1 in G2 is abolished when heterochromatin protein 1 is not bound to centromeric heterochromatin. Thus, it seems that Sgo1 sets up the centromeric protection mechanism in G2, but that its Bub1-dependent localisation to centromeres during mitosis is not required to maintain cohesion.

Key words: Mitosis, Kinetochore, Spindle-assembly checkpoint, BubR1, Cohesion

Introduction

The spindle-assembly checkpoint (SAC) delays anaphase onset until all the chromosomes are stably attached to spindle microtubules via their kinetochores (Musacchio and Salmon, 2007). It has long been appreciated that protein phosphorylation is involved in SAC regulation (Minshull et al., 1994; Nicklas et al., 1995). One of the first protein kinases identified as a SAC component was Bub1 (Roberts et al., 1994); since then, several other kinases have been implicated in SAC function, including Mps1, BubR1, Aurora B and others (Burke and Stukenberg, 2008).

Early evidence suggested that the kinase activity of Bub1 is required for SAC function. A Bub1 kinase mutant (*bub1-K733R*) failed to complement the benomyl sensitivity exhibited by a *bub1Δ* strain (Roberts et al., 1994). However, this mutation destabilises Bub1 in budding yeast (Warren et al., 2002). Surprisingly, a mutant completely lacking the kinase domain is checkpoint proficient (Fernius and Hardwick, 2007), suggesting that the kinase activity of Bub1 is not required for SAC function. In fission yeast, both *bub1-K762R* and a mutant lacking the entire kinase domain failed to prevent cell division in response to the microtubule toxin carbendazim, arguing that Bub1 activity is required for checkpoint function (Yamaguchi et al., 2003). Note that this mutant, which is equivalent to K733R in *Saccharomyces cerevisiae*, is a stable protein in *Schizosaccharomyces pombe*. However, a more recent study showed that a *bub1-K762M* strain was benomyl resistant (Vanoosthuyse et al., 2004), arguing that the catalytic activity of Bub1 is not essential for SAC signalling in *S. pombe*.

In *Xenopus* egg extracts, a catalytically inactive Bub1^{K872R} protein was capable of restoring checkpoint function, at least in response to high numbers of sperm nuclei (Sharp-Baker and Chen, 2001). However, a mutant lacking the kinase domain altogether was less efficient at sustaining the checkpoint when low numbers of nuclei were added (Chen, 2004), indicating that the catalytic activity of Bub1 might amplify a weak signal generated by just a few kinetochores.

On balance, observations from yeast and *Xenopus* argue that the kinase activity of Bub1 is not essential for SAC signalling. However, human Bub1 can inhibit the anaphase-promoting complex/cyclosome (APC/C) when bound to Cdc20, at least in vitro; by contrast, the kinase mutant Bub1^{K821A} cannot (Tang et al., 2004a). This inhibition might be direct, as Bub1 can phosphorylate Cdc20 in vitro. Interestingly, a non-phosphorylatable Cdc20 mutant exerted a partial dominant-negative effect on the checkpoint (Tang et al., 2004a). Despite in vitro evidence linking Bub1 to Cdc20, there is, however, no compelling evidence that Bub1 kinase activity is actually required for SAC function in mammalian cells. Indeed, the ability of Bub1 to restrain APC/C activity during the first meiotic division in mouse oocytes appears to be completely independent of its kinase domain (McGuinness et al., 2009), arguing that, as in other model systems, the kinase activity of Bub1 is not a key contributor to SAC signalling in mammals. Furthermore, a recent report showed that expression of a kinase-dead Bub1 or a mutant lacking the entire kinase domain restored the checkpoint, albeit partially, after Bub1 knockdown in HeLa cells (Klebig et al., 2009).

If the catalytic activity of Bub1 is not required for SAC function, what role does it play? From yeast to mammalian cells, Bub1 deficiency causes chromosome alignment and segregation errors that cannot simply be ascribed to SAC dysfunction (Bernard et al., 2001; Johnson et al., 2004; Meraldi and Sorger, 2005; Warren et

al., 2002), so perhaps its activity is required for another aspect of kinetochore and/or centromere function. In *S. pombe*, Bub1 recruits Sgo1 to centromeres to ensure that sister chromatids do not prematurely separate during meiosis I; there are, however, conflicting reports as to whether this requires Bub1 kinase activity (Kitajima et al., 2004; Vaur et al., 2005). The kinase domain does, however, appear to be required for Sgo2 function, thereby ensuring that sister kinetochores attach to the same spindle pole in meiosis I (Vaur et al., 2005). In budding yeast, the Bub1 kinase domain is required to recruit Sgo1 to centromeres to ensure that sister kinetochores attach to opposite poles during mitosis (Fernius and Hardwick, 2007). Bub1 is also required for centromeric localisation of Sgo1 in mammalian cells (Kitajima et al., 2005; Tang et al., 2004b). Recently, a Bub1 kinase deletion mutant was shown to impair loading of Sgo1 onto kinetochores in an RNAi-based complementation assay; this mutant was also unable to rescue chromosome alignment defects associated with Bub1 knockdown (Klebig et al., 2009). These observations are, however, complicated for two reasons: one, incomplete penetrance of the RNAi; and two, the complementing transgenes did not restore Bub1 to the levels observed in unperturbed cells.

To rigorously address the role of Bub1 kinase activity in mammalian cells, we established a complementation assay amenable to structure-function studies. We have previously described a system in which the *BUB1* gene could be efficiently inactivated in mouse embryo fibroblasts (MEFs). This generates bona fide *BUB1*-null cells, leading to SAC override and massive chromosome alignment defects (Perera et al., 2007). We also showed that the SAC defect could be rescued by transducing the cells with an adenovirus encoding a wild-type Bub1 cDNA (Perera et al., 2007). Here, we used this system to probe the role of Bub1 kinase activity in SAC function, chromosome alignment and Sgo1 recruitment.

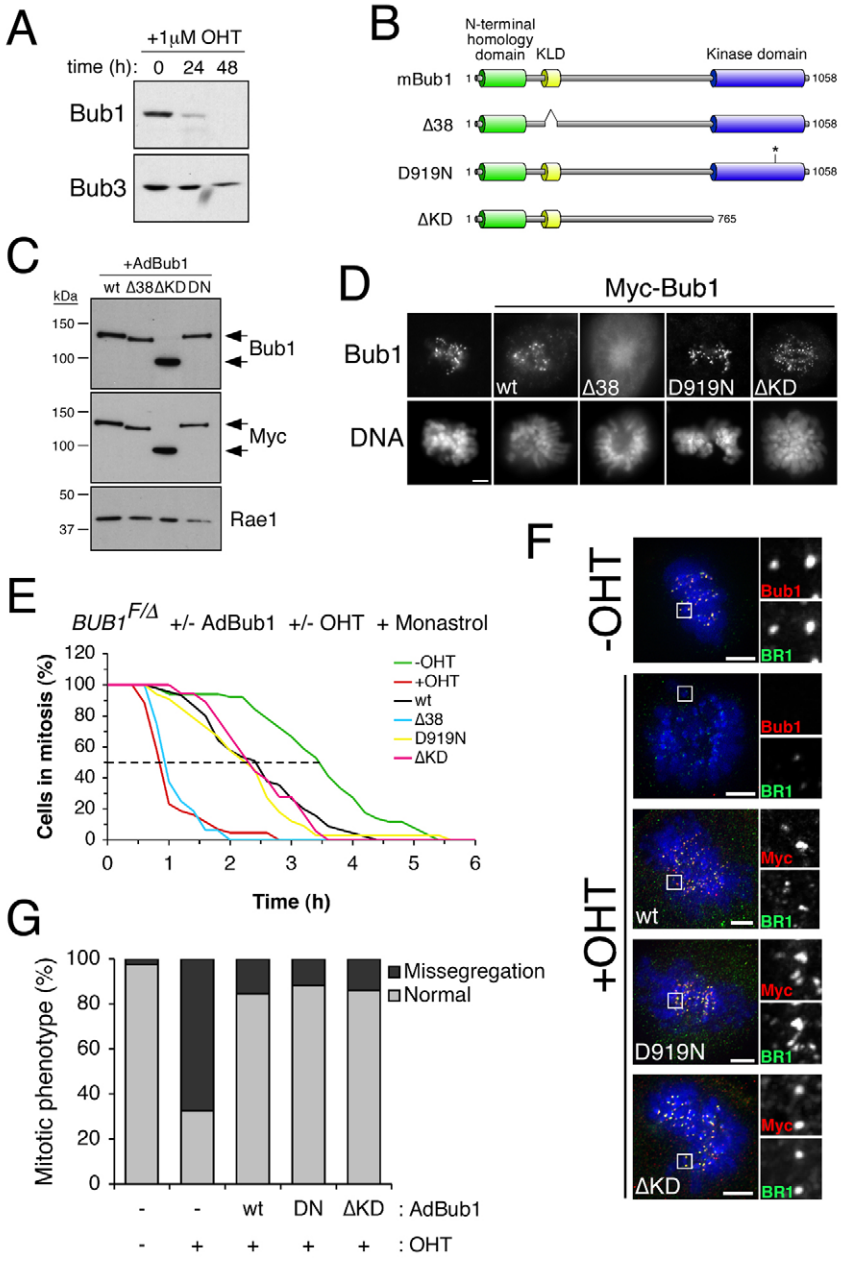

Fig. 1. Bub1 kinase activity is not required for the SAC or chromosome segregation. (**A**) Western blots of *BUB1*$^{F/Δ}$ *ER*^{T}*-Cre* iMEFs treated with 1 μM OHT for the indicated times, and then probed with Bub1 and Bub3 antibodies. (**B**) Diagram depicting the various Bub1 constructs used in this study. Numbers represent amino acid residues. The asterisk marks the point mutation in the D919N protein. KLD, kinetochore localisation domain. (**C**) Western blots of *BUB1*$^{F/Δ}$ *ER*^{T}*-Cre* iMEFs infected with adenoviruses encoding the indicated Bub1 constructs, and then probed for Bub1, Myc and Rae1. (**D**) Immunofluorescence images of iMEFs uninfected or infected with adenoviruses encoding the different Bub1 constructs. Cells were stained with an anti-Bub1 antibody to detect endogenous Bub1 or with an anti-Myc antibody to detect the exogenous proteins, and counterstained with Hoechst to visualise the DNA. Scale bar: 5 μm. (**E**) Line graphs plotting the percentage of cells in mitosis in the presence of monastrol. Asynchronous *BUB1*$^{F/Δ}$ *ER*^{T}*-Cre* MEFs were preinfected with adenoviruses as indicated and then treated with 0.5 μM OHT for 24 hours. The time in mitosis is defined as the interval between nuclear envelope breakdown and chromosome decondensation, as determined by phase-contrast time-lapse analysis. At least 16 cells were analysed for each condition. The dotted line marks the time at which 50% of the cells have exited mitosis for each condition. (**F**) Projections of deconvolved image stacks, showing that kinetochore localisation of BubR1 does not require Bub1 kinase activity. Asynchronous *BUB1*$^{F/Δ}$ *ER*^{T}*-Cre* MEFs were treated with 0.5 μM OHT and infected with adenoviruses as indicated for 24 hours, then fixed and stained for Bub1 (red), BubR1 (BR1, green) and DNA (blue). When infected with adenoviruses, cells were stained with an anti-Myc antibody (red) to detect the exogenous protein. Scale bars: 5 μm. (**G**) Bar graph quantifying the percentage of mitotic cells exhibiting chromosome mis-segregation. GFP-H2B-expressing *BUB1*$^{F/Δ}$ *ER*^{T}*-Cre* iMEFs were preinfected with adenoviruses as indicated, then treated with 1 μM OHT for 24 hours and analysed by fluorescence time-lapse microscopy.

Results and Discussion

We recently generated a mouse strain in which exons 7 and 8 of the *BUB1* gene, which encode the Bub3-binding domain (Taylor et al., 1998), were flanked with *loxP* sites to create the floxed allele $BUB1^{F}$ (flanked by *loxP*) (Perera et al., 2007). Mice harbouring $BUB1^{F}$ were crossed with a Cre-deleter strain to create $BUB1^{\Delta}$, which we showed to be a null allele (Perera et al., 2007). By crossing with a strain harbouring ER^{T}-*Cre*, a transgene that encodes a tamoxifen-responsive Cre recombinase (Hayashi and McMahon, 2002), we created $BUB1^{F/\Delta}$ and $BUB1^{F/+}$ embryos harbouring ER^{T}-*Cre*. Primary MEFs were prepared and, upon exposure to 4-hydroxy-tamoxifen (OHT), $BUB1^{F/\Delta}$ and $BUB1^{F/+}$ cells were efficiently converted to $BUB1^{\Delta/\Delta}$ and $BUB1^{\Delta/+}$ cells, respectively (Perera et al., 2007). We showed that, whereas the $BUB1^{\Delta/+}$ MEFs were phenotypically normal, $BUB1^{\Delta/\Delta}$ cells were checkpoint defective and failed to align their chromosomes. Because primary mouse fibroblasts rapidly undergo senescence in culture (Rohme, 1981) and are less amenable to transfection procedures, we created immortal MEFs (iMEFs) by transducing $BUB1^{F/\Delta}$ MEFs with a retrovirus encoding E1A/H-ras^{V12}. Importantly, exposing $BUB1^{F/\Delta}$ iMEFs to OHT led to efficient depletion of Bub1 protein (Fig. 1A).

To perform structure-function studies, we generated a series of recombinant adenoviruses constitutively expressing murine Bub1 cDNAs as N-terminal Myc-tagged fusions (Fig. 1B). As a positive control, we used a wild-type cDNA that we had previously showed could rescue the SAC defect in $BUB1^{\Delta/\Delta}$ cells (Perera et al., 2007). As a negative control, we used a Bub1 mutant lacking the Bub3-binding site (Bub1Δ38) (see Taylor et al., 1998) (Fig. 1B); we reasoned that, by not binding Bub3, this mutant should not be able to target the kinetochore and thereby not restore the kinetochore-related functions of Bub1. To probe the role of Bub1 kinase activity, we created two mutants (Fig. 1B). The first harbours a point mutation in the kinase domain, substituting the invariant aspartate at position 919 with asparagine, $Bub1^{D919N}$. This aspartate, in subdomain VII of the catalytic domain, is essential for the phospho-transfer reaction, chelating magnesium and orienting the β- and γ-phosphates of ATP (Hanks and Hunter, 1995). The second mutant, Bub1ΔKD, lacks the entire kinase domain.

To verify that the adenoviruses expressed proteins with the expected characteristics, we infected $BUB1^{F/\Delta}$ iMEFs, and then analysed them by immunoblotting and immunofluorescence. Importantly, each virus expressed apparently stable proteins, of the expected size, detected by antibodies against both the Myc tag and Bub1 (Fig. 1C). Note that the Myc-tagged Bub1 proteins are overexpressed relative to endogenous Bub1; the endogenous protein is therefore not detectable on these immunoblots. Whereas wild-type Myc-Bub1 targeted kinetochores in mitotic cells (Fig. 1D), the Bub1Δ38 mutant did not, consistent with previous observations demonstrating that Bub3 binding and kinetochore localisation are synonymous (Taylor et al., 1998). Importantly, both the $Bub1^{D919N}$ mutant and Bub1ΔKD also localised to kinetochores in mitosis. Thus, unlike the situation in budding yeast, point mutations in the kinase domain of murine Bub1 do not destabilise the protein.

To determine whether the Bub1 transgenes could rescue the SAC defect exhibited by *BUB1*-null cells, $BUB1^{F/\Delta}$ MEFs were transduced with Bub1 adenoviruses, treated with OHT to inactivate *BUB1* and then exposed to monastrol to prevent the formation of bipolar spindles. The cells were then analysed by phase-contrast time-lapse imaging to determine the length of time from nuclear envelope breakdown to chromosome decondensation. To compare

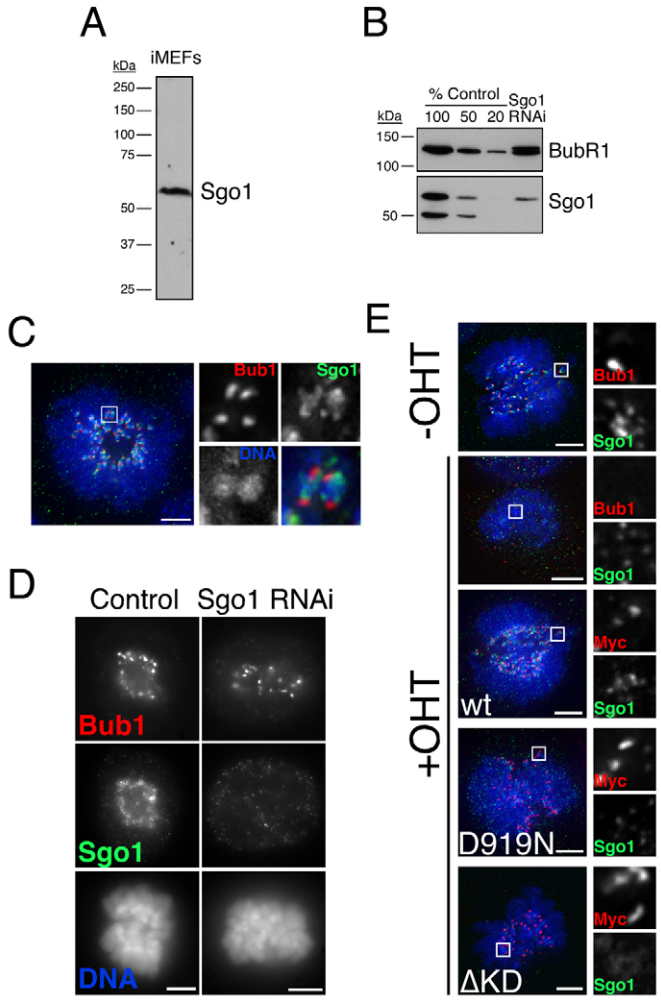

Fig. 2. Bub1 kinase activity is required for centromeric localisation of Sgo1 in mitosis. (**A**) Western blot of whole-cell extract from $BUB1^{F/\Delta}$ ER^{T}-*Cre* iMEFs probed with anti-Sgo1 antibody. (**B**) Western blots of HeLa cells treated with scrambled (control) or Sgo1 siRNAs, probed with anti-BubR1 and -Sgo1 antibodies. (**C**) Projection of deconvolved image stacks of a mitotic $BUB1^{F/\Delta}$ ER^{T}-*Cre* MEF stained for Bub1 (red), Sgo1 (green) and DNA (blue). The boxed region is enlarged in the panels on the right. Scale bar: 5 µm. (**D**) Immunofluorescence images of mitotic NIH/3T3 cells transfected with siRNA duplexes designed to repress murine Sgo1, fixed 48 hours later and stained as in C. Scale bars: 5 µm. (**E**) Projections of deconvolved image stacks showing that centromeric localisation of Sgo1 depends on Bub1 kinase activity. Asynchronous $BUB1^{F/\Delta}$ ER^{T}-*Cre* MEFs were treated with 0.5 µM OHT and infected with adenoviruses as indicated for 24 hours, then fixed and stained as in C. When infected with adenoviruses, cells were stained with an anti-Myc antibody (red) to detect the exogenous protein. Scale bars: 5 µm.

the SAC response in each case, we determined the time by which 50% of the cells had exited mitosis, hereafter called the T_{50}. In the absence of OHT treatment, the Bub1-proficient MEFs mounted a robust SAC response, with a T_{50} of ~3.5 hours (Fig. 1E). By contrast, inactivation of *BUB1* reduced the T_{50} to ~55 minutes. Transduction of wild-type Myc-Bub1 rescued the SAC defect, restoring the T_{50} to ~2.5 hours. Importantly, the Bub1Δ38 mutant did not restore SAC function, with the T_{50} remaining at ~60 minutes (Fig. 1E), confirming that Bub1 does need to bind Bub3 and/or localise to kinetochores to contribute to checkpoint signalling.

Consistent with previous observations in budding yeast, fission yeast and mouse oocytes, Bub1ΔKD did restore SAC function, with a T_{50} of ~2.5 hours (Fig. 1E). Although this does not represent complete rescue, the Bub1ΔKD mutant is as competent as wild-type Myc-Bub1. Bub1^{D919N} also restored SAC function to the same extent as wild-type Bub1 and Bub1ΔKD, suggesting that the kinase activity of Bub1 is not required for the SAC. Furthermore, both wild-type Bub1 and the kinase mutants restored kinetochore localisation of BubR1, a downstream SAC component (Fig. 1F). Thus, these results are in agreement with reports using other model organisms (Fernius and Hardwick, 2007; Sharp-Baker and Chen, 2001; Vanoosthuyse et al., 2004).

A key issue is why the wild-type transgene did not result in complete rescue. One possibility is that transgene overexpression induces dominant-negative effects. We suspect that this is not the case; when we overexpressed the wild-type or D919N constructs in the presence of endogenous Bub1, SAC function appeared normal (supplementary material Fig. S1). Another possibility is interference caused by the Myc tag. Although we cannot rule this out, it seems unlikely because wild-type Myc-Bub1 restored kinetochore localisation of BubR1 to levels seen in controls (Fig. 1F and supplementary material Fig. S2A). A more likely possibility is incomplete transduction; when we analysed cells by immunofluorescence, ~20% of the mitotic cells did not show Myc-positive kinetochores (data not shown). With respect to BubR1, although the vast majority of Bub1-deficient cells lacked BubR1 at kinetochores, we sometimes noticed faint kinetochore localisation in the apparent absence of Bub1. One possibility is that these cells still have some Bub1 left; even though the gene was deleted, it might take several cell cycles to degrade all the protein (Fig. 1A). Alternatively, BubR1 can perhaps be recruited – albeit very inefficiently – via a direct interaction with blinkin (Kiyomitsu et al., 2007). Nevertheless, taking into account numerous reports (Boyarchuk et al., 2007; Jeganathan et al., 2007; Johnson et al., 2004; Wong and Fang, 2006), it appears that Bub1 is required to recruit BubR1 to kinetochores.

Next, we asked whether Bub1^{D919N} or the Bub1ΔKD mutant could restore chromosome alignment. For this purpose, we generated iMEFs stably expressing GFP-tagged histone H2B in order to visualise the chromatin. Consistent with our previous analysis of primary MEFs, OHT-mediated inactivation of *BUB1* in the iMEFs dramatically affected chromosome alignment and segregation (data not shown); whereas 97% of control cells completed mitosis apparently normally, 67% of the Bub1-deficient iMEFs underwent aberrant mitosis (Fig. 1G). Note that this alignment defect was not simply due to SAC override; when *BUB1*-null iMEFs were treated with the proteasome inhibitor MG132 to block entry into anaphase, unaligned chromosomes were still apparent (data not shown) (see Perera et al., 2007). When the *BUB1*-null iMEFs were reconstituted with wild-type Bub1, chromosome alignment and segregation were apparently normal in 85% of cells, indicating efficient rescue of the null phenotype (Fig. 1G). Significantly, both Bub1^{D919N} and the Bub1ΔKD mutant also restored chromosome segregation, with 88% and 86% of the cells undergoing normal mitosis, respectively (Fig. 1G). Thus, the kinase activity of Bub1 does not appear to be required for chromosome alignment in mouse fibroblasts.

Interestingly, a recent report showed that Bub1 kinase mutants were unable to rescue the chromosome alignment defect induced by RNAi-mediated knockdown of Bub1 in HeLa cells (Klebig et al., 2009). This represents a clear discrepancy: in our studies, the kinase activity of Bub1 is not required for chromosome alignment, whereas it is according to Klebig et al. However, note that, in the previous study (Klebig et al., 2009), the transgenes expressing the kinase mutants did not restore Bub1 levels to those observed in control cells; we estimate that the Bub1ΔKD mutant, for example, was expressed to only ~50% of endogenous expression levels [see figure 3E in Klebig et al. (Klebig et al., 2009)]. Importantly, it is clear that partial repression of Bub1 compromises chromosome alignment, whereas more extensive repression is required for SAC override (Johnson et al., 2004; Meraldi and Sorger, 2005). We suggest, therefore, that the incomplete restoration of Bub1 was sufficient to restore SAC function, but not chromosome alignment. By contrast, in our study, the adenoviral vectors overexpress Bub1 relative to endogenous protein (Fig. 1C), thus achieving an expression level capable of complementing both SAC and alignment functions. In summary, when Bub1 kinase mutants are transduced into bona fide *BUB1*-null cells to levels greater than endogenous, both SAC function and chromosome alignment are restored, indicating that Bub1 kinase activity is not essential for either function, at least under our experimental conditions. Importantly, we cannot rule out the possibility that Bub1 activity is required under conditions not revealed by our assays. For example, perhaps Bub1 activity is more important in certain developmental contexts or in response to specific stresses. Alternatively, Bub1 activity might be more important for fine-tuning the SAC; for example, in response to one or two unattached kinetochores, perhaps Bub1 activity amplifies a weak SAC signal. Indeed, although consistent with previous reports, because of the caveats outlined above, our experiments are not necessarily definitive and additional efforts will be required to determine whether Bub1 activity plays a role in fine-tuning the SAC.

If the kinase activity of Bub1 is not required for SAC function or chromosome alignment, what role does it play? The kinase activity of Bub1 has been implicated in the recruitment of Sgo1 to centromeres and/or kinetochores in budding yeast and *Xenopus* egg extracts (Boyarchuk et al., 2007; Fernius and Hardwick, 2007; Riedel et al., 2006). We therefore decided to analyse the recruitment of Sgo1 in *BUB1*-null cells expressing Bub1 kinase mutants. Previously, using an already described reagent (Tang et al., 2004b), we showed that an antibody against human Sgo1 decorated kinetochores in primary MEFs and that this pattern was Bub1 dependent (Perera et al., 2007). However, Sgo1 has been reported to localise to centromeres rather than to kinetochores (McGuinness et al., 2005). Therefore, we generated a novel antibody against mouse Sgo1. This antibody recognised a single major band in extracts prepared from iMEFs (Fig. 2A). Consistent with there being multiple human Sgo1 isoforms (McGuinness et al., 2005), this antibody detected two bands in HeLa cells, both of which diminished following transfection of small interfering (si)RNA duplexes designed to repress Sgo1 (Fig. 2B). When used to stain iMEFs, the anti-Sgo1 antibody decorated mitotic chromosomes, with the signal concentrating near Bub1-positive foci during the early stages of mitosis, indicative of centromeres and/or kinetochores (supplementary material Fig. S3). By late anaphase, the Sgo1 foci were no longer apparent (supplementary material Fig. S3). Closer inspection revealed that, in prometaphase, the Sgo1 signal was located between the Bub1 foci, consistent with enrichment at centromeres (Fig. 2C). Importantly, this signal diminished following Sgo1 RNAi, confirming the specificity of the antibody (Fig. 2D).

In Bub1-deficient prometaphase iMEFs, the centromeric Sgo1 signal was greatly reduced (Fig. 2E). However, when we

reconstituted cells with wild-type *BUB1* cDNA, centromeric localisation of Sgo1 was restored, arguing that Bub1 is indeed required for Sgo1 localisation in mitosis. Strikingly, neither Bub1^{D919N} nor the Bub1ΔKD mutant was capable of restoring Sgo1 at centromeres (Fig. 2E and supplementary material Fig. S2B), indicating that, in mouse fibroblasts, Bub1 kinase activity is required for centromeric localisation of Sgo1, consistent with results in budding yeast, *Xenopus* egg extracts and HeLa cells (Boyarchuk et al., 2007; Fernius and Hardwick, 2007; Klebig et al., 2009; Riedel et al., 2006). Note, however, that the inability of Sgo1 to localise to centromeres in Bub1-deficient cells does not result in premature loss of sister chromatid cohesion (Perera et al., 2007) or obvious chromosome mis-segregation (Fig. 1G and data not shown). These results suggest that Sgo1 localisation at centromeres during mitosis is not essential for maintaining cohesion, SAC function or chromosome alignment.

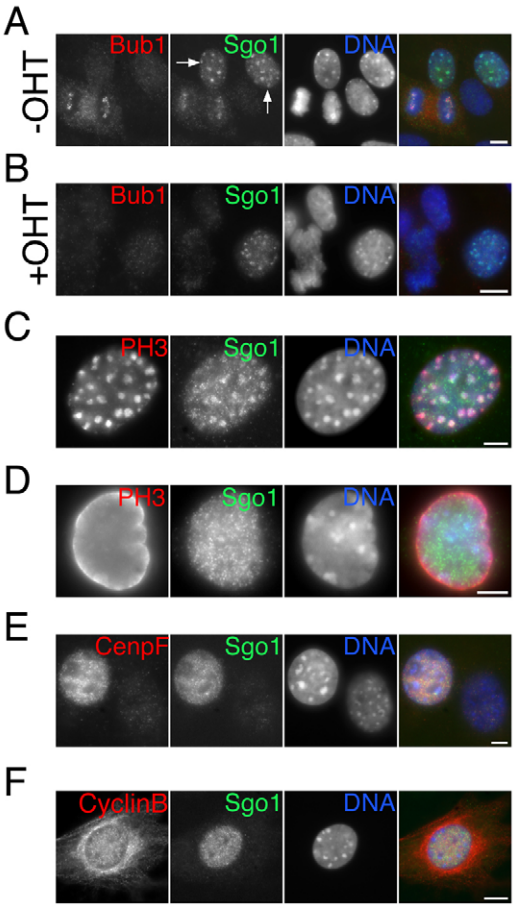

Fig. 3. Sgo1 localises to pericentric heterochromatin in G2. (**A**) Immunofluorescence images of *BUB1*$^{F/Δ}$ *ER*^{T}*-Cre* iMEFs stained for Bub1 (red), Sgo1 (green) and DNA (blue), showing heterochromatin staining of Sgo1 in two interphase cells with no detectable Bub1 signal (arrows). Scale bar: 20 µm. (**B**) Immunofluorescence images of *BUB1*$^{F/Δ}$ *ER*^{T}*-Cre* iMEFs treated with 1 µM OHT for 24 hours, then fixed and stained as in A. Scale bar: 10 µm. (**C**) Immunofluorescence images of an NIH/3T3 cell stained for phospho-H3 (PH3, red), Sgo1 (green) and DNA (blue). Scale bar: 5 µm. (**D**) Immunofluorescence images of an NIH/3T3 cell stained as in C. Scale bar: 5 µm. (**E**) Immunofluorescence images of NIH/3T3 cells stained for Cenp-F (red), Sgo1 (green) and DNA (blue). Scale bar: 5 µm. (**F**) Immunofluorescence images of a 10T1/2 cell stained for cyclin B1 (red), Sgo1 (green) and DNA (blue). Scale bar: 5 µm.

This presents a paradox; if Sgo1 is required to maintain centromeric cohesion during prometaphase, why does dislodging it from centromeres not induce a premature loss of cohesion in our assays, as observed following Sgo1 RNAi (McGuinness et al., 2005; Tang et al., 2004b)? Interestingly, during the course of our analysis, we noticed that the Sgo1 antibody stained Hoechst-dense heterochromatin regions in interphase nuclei, preceding the appearance of Bub1 at kinetochores (Fig. 3A). This staining does indeed seem to represent Sgo1, as a similar pattern manifests in cells transfected with either GFP-tagged or Myc-tagged Sgo1

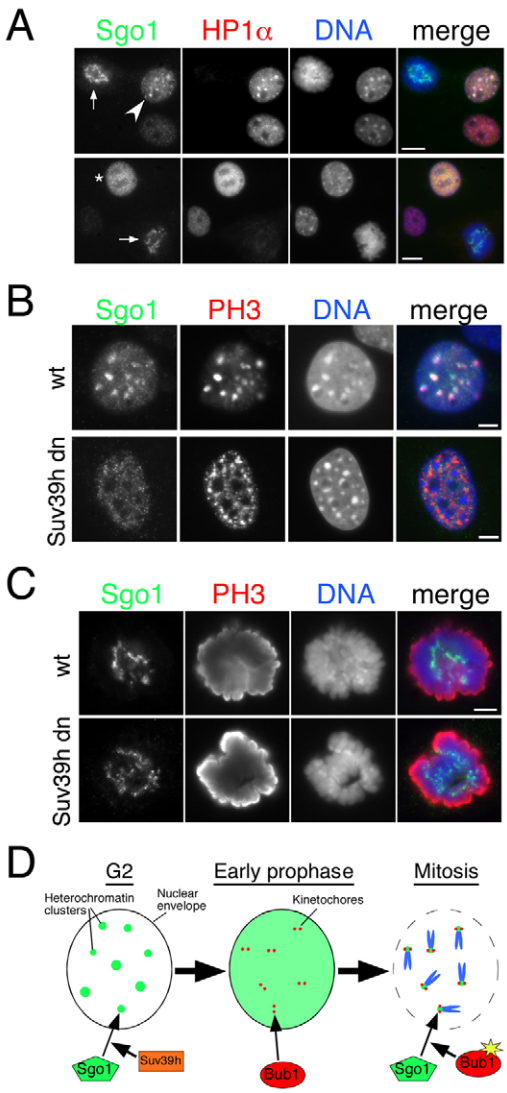

Fig. 4. Localisation of Sgo1 in G2, but not mitosis, depends on the Suv39h-HP1 pathway. (**A**) Immunofluorescence images of NIH/3T3 cells stained for Sgo1 (green), HP1α (red) and DNA (blue). Arrows indicate mitotic cells. The arrowhead indicates a cell with Sgo1- and HP1α-positive foci. The asterisk indicates an interphase cell with strong homogeneous nuclear Sgo1 staining and no detectable HP1α foci. Scale bars: 10 µm. (**B**) Immunofluorescence images of wild-type (wt) and Suv39h double-null (dn) interphase MEFs stained for Sgo1 (green), phospho-H3 (PH3, red) and DNA (blue). Scale bars: 5 µm. (**C**) Immunofluorescence images of wild-type (wt) and Suv39h double-null (dn) mitotic MEFs stained as in B. Scale bar: 5 µm. (**D**) Model depicting the two-step recruitment of Sgo1 at the G2-to-M transition, as described in this study. See text for details.

(supplementary material Fig. S4A,B) and disappears after RNAi-mediated repression of Sgo1 (supplementary material Fig. S4C). Importantly, Sgo1-positive foci were apparent even in Bub1-deficient iMEFs (Fig. 3B and supplementary material Fig. S4D), indicating that the recruitment of Sgo1 to heterochromatin is Bub1 independent. In the majority of cells, the Sgo1 foci also stained positive for histone H3 phosphorylated at serine 10 (phospho-H3^{Ser10}), a post-translational modification that starts in pericentric heterochromatin during early G2 (Fig. 3C and supplementary material Fig. S4E), suggesting that these cells are in G2 (Hendzel et al., 1997). However, some cells showed a more diffuse nuclear Sgo1 signal, without any major detectable foci (Fig. 3D). These cells typically displayed strong homogeneous nuclear staining for phospho-H3^{Ser10} (Fig. 3D and supplementary material Fig. S4E), Cenp-F was abundant in the nucleus (Fig. 3E and supplementary material Fig. S4F) and cyclin B1 was abundant in the cytoplasm (Fig. 3F), indicating that they were in late G2 or early prophase (Hendzel et al., 1997; Hussein and Taylor, 2002; Pines and Hunter, 1991).

Localisation of Sgo1 at pericentric heterochromatin has been described in budding and fission yeast (Kiburz et al., 2005; Yamagishi et al., 2008). Indeed, in *S. pombe* heterochromatin protein 1α (HP1α), which localises to pericentric heterochromatin, interacts with Sgo1 and is required for its localisation at centromeres during mitosis (Yamagishi et al., 2008). This report also showed that HP1α localised to mitotic centromeres in human cells and was required to recruit Sgo1. This is, however, at odds with reports showing that HP1α dissociates from centromeres in prophase (Fischle et al., 2005; Hirota et al., 2005). Furthermore, although Sgo1 interacts with all three human HP1 isoforms (Serrano et al., 2009), repression of HP1 by RNAi apparently did not dislodge Sgo1 from mitotic centromeres in HeLa cells. To explain these discrepancies, we wondered whether G2 recruitment of Sgo1 might be HP1 dependent, whereas later mitotic recruitment might be HP1 independent. Consistent with this notion, we found that 91% of cells with Sgo1-positive foci also stained positive for HP1α foci and that these foci colocalised, confirming the heterochromatin localisation of Sgo1 (Fig. 4A). However, HP1α foci were not present in cells with nuclear Sgo1 staining (Fig. 4A), again consistent with the notion that these cells are in very late G2 or early prophase. To determine whether HP1 is required for heterochromatin localisation of Sgo1 in G2, we analysed mouse fibroblasts lacking both genes encoding the Suv39h methyltransferase (Peters et al., 2001). In these cells, histone H3 is not trimethylated on lysine 9 (H3K9me3) and thus HP1 is not recruited to heterochromatin (Guenatri et al., 2004; Peters et al., 2001). Significantly, pericentric heterochromatin localisation of Sgo1 during G2 was abolished in Suv39h double-null MEFs (Fig. 4B and supplementary material Fig. S4G). This result indicates that the recruitment of Sgo1 to heterochromatin in G2 is dependent on the H3K9me3-HP1 pathway. However, centromeric localisation of Sgo1 during mitosis was not affected in Suv39h double-null MEFs (Fig. 4C), in agreement with our results showing that mitotic localisation of Sgo1 is dependent on Bub1 catalytic activity.

In summary, our data indicate that Sgo1 exhibits three different localisations during the later stages of the cell cycle (Fig. 4D). In early to mid G2, Sgo1 localises to pericentric heterochromatin in an HP1-dependent, Bub1-independent manner. Then, in late G2 to early prophase, as HP1 dissociates from centromeres (Fischle et al., 2005; Hirota et al., 2005), Sgo1 becomes more diffuse throughout the nucleus. At the onset of mitosis, Sgo1 is targeted back to centromeres, in a manner that is dependent on Bub1 kinase activity. We propose that it is this initial recruitment of Sgo1 to pericentric heterochromatin in G2 that is required to establish the centromeric cohesion protection mechanism. Indeed, two independent reports show that, when mitotic chromosomes are prepared from Suv39h double-null MEFs, they appear to have lost centromeric cohesion prematurely (Guenatri et al., 2004; Koch et al., 2008). Note that, although the Suv39h double-null MEFs display chromosome instability, they are, however, viable; we suspect that this is probably because the residual cohesin at chromosome arms provides sufficient sister chromatid cohesion for long enough to allow chromosome alignment [see figures 7 and 5 in Guenatri et al. and Koch et al., respectively (Guenatri et al., 2004; Koch et al., 2008)]. Importantly, this new model explains why Bub1 catalytic activity is not required to maintain centromeric cohesion (Perera et al., 2007), even though it is clearly required to recruit Sgo1 to centromeres in mitosis.

Materials and Methods

Cell culture and drug treatments

MEFs from 13.5-day-old embryos were prepared and cultured as described previously (Perera et al., 2007). To activate Cre, MEFs were cultured in optiMEM media (Invitrogen) plus 10% charcoal-dextran-treated serum (Hyclone); OHT (Sigma, 10 mg/ml stock in ethanol) was added at 0.5-1.0 μM. NIH/3T3 and 10t1/2 cells were obtained from the ATCC and cultured in DMEM plus 10% fetal calf serum, 100 U/ml penicillin, 100 μg/ml streptomycin and 2 mM glutamine (Invitrogen). For the generation of iMEF lines, a pLPC-E1A-ires-Hras^{V12} plasmid (kind gift from Manuel Serrano, CNIO, Madrid, Spain) was used to generate retroviruses in Phoenix-Eco packaging cells (purchased from the ATCC). Viruses were then used to infect MEFs as described and surviving clones were selected with 0.5 μg/ml puromycin (Sigma). A cDNA encoding GFP-tagged histone H2B (Morrow et al., 2005) was cloned into pLNCX2 and used to generate retroviruses as above. These retroviruses were used to infect iMEFs, which were subsequently selected with 0.75 mg/ml G418 (Sigma). NIH/3T3 cells were transfected using the calcium phosphate method. RNAi was performed in NIH/3T3 cells by transfection of ON-TARGET-plus SMART pool siRNAs targeting mouse Sgo1 (Thermo Scientific), using interferin (Polyplus Transfection). MG132 and monastrol (Sigma) were used at 20 μM and 100 μM final concentrations, respectively.

Generation of Bub1 mutants and adenovirus

The *Bub1*^{D919N} allele was generated by a single-base substitution (guanine to adenine) in full-length mouse *BUB1* cDNA cloned into pcDNA3/Myc using site-directed mutagenesis (Stratagene). The *Bub1ΔKD* allele was generated by PCR amplification of the region encoding amino acids 1 to 765. The *Bub1Δ38* allele lacks the Bub3-binding region (amino acids 241 to 278) and has been described previously (Taylor et al., 1998). All Myc-tagged mouse Bub1 transgenes were subcloned into a pShuttleCMV vector as *Bgl*II-*Not*I digests. This vector was used to generate recombinant adenoviruses using the AdEasy system (Stratagene), according to the manufacturer's instructions. MEF cultures were infected with a multiplicity of infection of ~100.

Generation of anti-Sgo1 antibody

An antibody against the N terminus of mouse Sgo1 was raised in rabbits. Briefly, the cDNA encoding amino acids 1 to 166 of mouse Sgo1 (GenBank accession number AB193067.1) was cloned into pGEX-4T-3 (GE Healthcare) and the GST-fusion protein, purified from *Escherichia coli* BL21 cells, was used to immunize a rabbit following standard procedures (PTU/BS, Scotland). Specific antibodies were obtained from the immune serum by affinity purification using the antigen coupled to glutathione-sepharose beads. To test the specificity of the purified antibody, Sgo1 was repressed in HeLa cells following standard procedures (Johnson et al., 2004), using siRNA duplexes described previously (Salic et al., 2004).

Cell biology

For immunoblotting, proteins were extracted in a lysis buffer containing 10 mM Tris pH 7.4, 100 mM NaCl, 1 mM EDTA, 1 mM EGTA, 0.1% Triton X-100, 10 mM β-glycerophosphate, 1 mM DTT, 0.2 mM PMSF and protease inhibitors, separated by SDS-PAGE, transferred to nitrocellulose membranes, blocked in TBST (50 mM Tris pH 7.6, 150 mM NaCl, 0.1% Tween-20) plus 5% non-fat dried milk, and probed with the following antibodies: SB1.3 [sheep anti-Bub1, 1:1000 (Taylor et al., 2001)], SBR1.1 [sheep anti-BubR1, 1:1000 (Taylor et al., 2001)], 4A6 (mouse anti-Myc, 1:5000; Millipore), SB3.2 (sheep anti-Bub3, 1:250; Andrew Holland and S.S.T, unpublished), SR1.2 (sheep anti-Rae1, 1:1000; Andrew Holland and S.S.T., unpublished) and RSG1 (rabbit anti-Sgo1, 1:500; this study). HRP-conjugated secondary antibodies were purchased from Zymed. For immunofluorescence analysis, cells were fixed in PBS plus 1% formaldehyde, permeabilised in 0.1% Triton X-100

and then stained with the following primary antibodies: 4B12 [mouse anti-Bub1, 1:20 (Taylor and McKeon, 1997)], SBR1.1 (1:1000), 4A6 (1:800), mouse anti-phospho-histone $H3^{Ser10}$ (1:500; ab14955, Abcam), SCF2 (sheep anti-mCenp-F, 1:500; Mailys Vergnolle and S.S.T., unpublished), mouse anti-cyclin-B1 (1:500; Millipore), mouse anti-HP1α (1:1000; Millipore) and RSG1 (1:100). Cy3- and Cy2-conjugated secondary antibodies were purchased from Jackson Immunoresearch Laboratories. Alexa-Fluor-488-conjugated secondary antibodies were from Molecular Probes. Widefield microscopy, deconvolution and imaging processing were all done as described (Taylor et al., 2001). Time-lapse microscopy was done as described previously (Morrow et al., 2005), acquiring images every 2 minutes for up to 24 hours. XY-point visiting was performed using a PZ-2000 automated stage (Applied Scientific Instrumentation).

The authors thank Manuel Serrano (CNIO, Madrid, Spain) for the kind gift of pLPC-E1A-ires-$Hras^{V12}$ plasmid and Thomas Jenuwein (MPI-IB, Freiburg, Germany) for providing the Suv39h double-null MEFs. We thank Janni Petersen and members of the Taylor laboratory for comments on the manuscript. D.P. is funded by Cancer Research UK, S.S.T. is a Cancer Research UK Senior Fellow.

Supplementary material available online at
http://jcs.biologists.org/cgi/content/full/123/5/653/DC1

References

Bernard, P., Maure, J. F. and Javerzat, J. P. (2001). Fission yeast Bub1 is essential in setting up the meiotic pattern of chromosome segregation. *Nat. Cell Biol.* **3**, 522-526.

Boyarchuk, Y., Salic, A., Dasso, M. and Arnaoutov, A. (2007). Bub1 is essential for assembly of the functional inner centromere. *J. Cell Biol.* **176**, 919-928.

Burke, D. J. and Stukenberg, P. T. (2008). Linking kinetochore-microtubule binding to the spindle checkpoint. *Dev. Cell* **14**, 474-479.

Chen, R. H. (2004). Phosphorylation and activation of Bub1 on unattached chromosomes facilitate the spindle checkpoint. *EMBO J.* **23**, 3113-3121.

Fernius, J. and Hardwick, K. G. (2007). Bub1 kinase targets Sgo1 to ensure efficient chromosome biorientation in budding yeast mitosis. *PLoS Genet.* **3**, e213.

Fischle, W., Tseng, B. S., Dormann, H. L., Ueberheide, B. M., Garcia, B. A., Shabanowitz, J., Hunt, D. F., Funabiki, H. and Allis, C. D. (2005). Regulation of HP1-chromatin binding by histone H3 methylation and phosphorylation. *Nature* **438**, 1116-1122.

Guenatri, M., Bailly, D., Maison, C. and Almouzni, G. (2004). Mouse centric and pericentric satellite repeats form distinct functional heterochromatin. *J. Cell Biol.* **166**, 493-505.

Hanks, S. K. and Hunter, T. (1995). Protein kinases 6. The eukaryotic protein kinase superfamily: kinase (catalytic) domain structure and classification. *FASEB J.* **9**, 576-596.

Hayashi, S. and McMahon, A. P. (2002). Efficient recombination in diverse tissues by a tamoxifen-inducible form of Cre: a tool for temporally regulated gene activation/inactivation in the mouse. *Dev. Biol.* **244**, 305-318.

Hendzel, M. J., Wei, Y., Mancini, M. A., Van Hooser, A., Ranalli, T., Brinkley, B. R., Bazett-Jones, D. P. and Allis, C. D. (1997). Mitosis-specific phosphorylation of histone H3 initiates primarily within pericentromeric heterochromatin during G2 and spreads in an ordered fashion coincident with mitotic chromosome condensation. *Chromosoma* **106**, 348-360.

Hirota, T., Lipp, J. J., Toh, B. H. and Peters, J. M. (2005). Histone H3 serine 10 phosphorylation by Aurora B causes HP1 dissociation from heterochromatin. *Nature* **438**, 1176-1180.

Hussein, D. and Taylor, S. S. (2002). Farnesylation of Cenp-F is required for G2/M progression and degradation after mitosis. *J. Cell Sci.* **115**, 3403-3414.

Jeganathan, K., Malureanu, L., Baker, D. J., Abraham, S. C. and van Deursen, J. M. (2007). Bub1 mediates cell death in response to chromosome missegregation and acts to suppress spontaneous tumorigenesis. *J. Cell Biol.* **179**, 255-267.

Johnson, V. L., Scott, M. I., Holt, S. V., Hussein, D. and Taylor, S. S. (2004). Bub1 is required for kinetochore localization of BubR1, Cenp-E, Cenp-F and Mad2, and chromosome congression. *J. Cell Sci.* **117**, 1577-1589.

Kiburz, B. M., Reynolds, D. B., Megee, P. C., Marston, A. L., Lee, B. H., Lee, T. I., Levine, S. S., Young, R. A. and Amon, A. (2005). The core centromere and Sgo1 establish a 50-kb cohesin-protected domain around centromeres during meiosis I. *Genes Dev.* **19**, 3017-3030.

Kitajima, T. S., Kawashima, S. A. and Watanabe, Y. (2004). The conserved kinetochore protein shugoshin protects centromeric cohesion during meiosis. *Nature* **427**, 510-517.

Kitajima, T. S., Hauf, S., Ohsugi, M., Yamamoto, T. and Watanabe, Y. (2005). Human Bub1 defines the persistent cohesion site along the mitotic chromosome by affecting Shugoshin localization. *Curr. Biol.* **15**, 353-359.

Kiyomitsu, T., Obuse, C. and Yanagida, M. (2007). Human Blinkin/AF15q14 is required for chromosome alignment and the mitotic checkpoint through direct interaction with Bub1 and BubR1. *Dev. Cell* **13**, 663-676.

Klebig, C., Korinth, D. and Meraldi, P. (2009). Bub1 regulates chromosome segregation in a kinetochore-independent manner. *J. Cell Biol.* **185**, 841-858.

Koch, B., Kueng, S., Ruckenbauer, C., Wendt, K. S. and Peters, J. M. (2008). The Suv39h-HP1 histone methylation pathway is dispensable for enrichment and protection of cohesin at centromeres in mammalian cells. *Chromosoma* **117**, 199-210.

McGuinness, B. E., Hirota, T., Kudo, N. R., Peters, J. M. and Nasmyth, K. (2005). Shugoshin prevents dissociation of cohesin from centromeres during mitosis in vertebrate cells. *PLoS Biol.* **3**, e86.

McGuinness, B. E., Anger, M., Kouznetsova, A., Gil-Bernabé, A. M., Helmhart, W., Kudo, N. R., Wuensche, A., Taylor, S., Hoog, C., Novak, B. et al. (2009). Regulation of APC/C activity in oocytes by a Bub1-dependent spindle assembly checkpoint. *Curr. Biol.* **19**, 369-380.

Meraldi, P. and Sorger, P. K. (2005). A dual role for Bub1 in the spindle checkpoint and chromosome congression. *EMBO J.* **24**, 1621-1633.

Minshull, J., Sun, H., Tonks, N. K. and Murray, A. W. (1994). A MAP kinase-dependent spindle assembly checkpoint in Xenopus egg extracts. *Cell* **79**, 475-486.

Morrow, C. J., Tighe, A., Johnson, V. L., Scott, M. I., Ditchfield, C. and Taylor, S. S. (2005). Bub1 and aurora B cooperate to maintain BubR1-mediated inhibition of APC/CCdc20. *J. Cell Sci.* **118**, 3639-3652.

Musacchio, A. and Salmon, E. D. (2007). The spindle-assembly checkpoint in space and time. *Nat. Rev. Mol. Cell. Biol.* **8**, 379-393.

Nicklas, R. B., Ward, S. C. and Gorbsky, G. J. (1995). Kinetochore chemistry is sensitive to tension and may link mitotic forces to a cell cycle checkpoint. *J. Cell Biol.* **130**, 929-939.

Perera, D., Tilston, V., Hopwood, J. A., Barchi, M., Boot-Handford, R. P. and Taylor, S. S. (2007). Bub1 maintains centromeric cohesion by activation of the spindle checkpoint. *Dev. Cell* **13**, 566-579.

Peters, A. H., O'Carroll, D., Scherthan, H., Mechtler, K., Sauer, S., Schofer, C., Weipoltshammer, K., Pagani, M., Lachner, M., Kohlmaier, A. et al. (2001). Loss of the Suv39h histone methyltransferases impairs mammalian heterochromatin and genome stability. *Cell* **107**, 323-337.

Pines, J. and Hunter, T. (1991). Human cyclins A and B1 are differentially located in the cell and undergo cell cycle-dependent nuclear transport. *J. Cell Biol.* **115**, 1-17.

Riedel, C. G., Katis, V. L., Katou, Y., Mori, S., Itoh, T., Helmhart, W., Galova, M., Petronczki, M., Gregan, J., Cetin, B. et al. (2006). Protein phosphatase 2A protects centromeric sister chromatid cohesion during meiosis I. *Nature* **441**, 53-61.

Roberts, B. T., Farr, K. A. and Hoyt, M. A. (1994). The Saccharomyces cerevisiae checkpoint gene BUB1 encodes a novel protein kinase. *Mol. Cell. Biol.* **14**, 8282-8291.

Rohme, D. (1981). Evidence for a relationship between longevity of mammalian species and life spans of normal fibroblasts in vitro and erythrocytes in vivo. *Proc. Natl. Acad. Sci. USA* **78**, 5009-5013.

Salic, A., Waters, J. C. and Mitchison, T. J. (2004). Vertebrate shugoshin links sister centromere cohesion and kinetochore microtubule stability in mitosis. *Cell* **118**, 567-578.

Serrano, A., Rodriguez-Corsino, M. and Losada, A. (2009). Heterochromatin protein 1 (HP1) proteins do not drive pericentromeric cohesin enrichment in human cells. *PLoS ONE* **4**, e5118.

Sharp-Baker, H. and Chen, R. H. (2001). Spindle checkpoint protein Bub1 is required for kinetochore localization of Mad1, Mad2, Bub3, and CENP-E, independently of its kinase activity. *J. Cell Biol.* **153**, 1239-1250.

Tang, Z., Shu, H., Oncel, D., Chen, S. and Yu, H. (2004a). Phosphorylation of Cdc20 by Bub1 provides a catalytic mechanism for APC/C inhibition by the spindle checkpoint. *Mol. Cell* **16**, 387-397.

Tang, Z., Sun, Y., Harley, S. E., Zou, H. and Yu, H. (2004b). Human Bub1 protects centromeric sister-chromatid cohesion through Shugoshin during mitosis. *Proc. Natl. Acad. Sci. USA* **101**, 18012-18017.

Taylor, S. S. and McKeon, F. (1997). Kinetochore localization of murine Bub1 is required for normal mitotic timing and checkpoint response to spindle damage. *Cell* **89**, 727-735.

Taylor, S. S., Ha, E. and McKeon, F. (1998). The human homologue of Bub3 is required for kinetochore localization of Bub1 and a Mad3/Bub1-related protein kinase. *J. Cell Biol.* **142**, 1-11.

Taylor, S. S., Hussein, D., Wang, Y., Elderkin, S. and Morrow, C. J. (2001). Kinetochore localisation and phosphorylation of the mitotic checkpoint components Bub1 and BubR1 are differentially regulated by spindle events in human cells. *J. Cell Sci.* **114**, 4385-4395.

Vanoosthuyse, V., Valsdottir, R., Javerzat, J. P. and Hardwick, K. G. (2004). Kinetochore targeting of fission yeast Mad and Bub proteins is essential for spindle checkpoint function but not for all chromosome segregation roles of Bub1p. *Mol. Cell. Biol.* **24**, 9786-9801.

Vaur, S., Cubizolles, F., Plane, G., Genier, S., Rabitsch, P. K., Gregan, J., Nasmyth, K., Vanoosthuyse, V., Hardwick, K. G. and Javerzat, J. P. (2005). Control of Shugoshin function during fission-yeast meiosis. *Curr. Biol.* **15**, 2263-2270.

Warren, C. D., Brady, D. M., Johnston, R. C., Hanna, J. S., Hardwick, K. G. and Spencer, F. A. (2002). Distinct chromosome segregation roles for spindle checkpoint proteins. *Mol. Biol. Cell* **13**, 3029-3041.

Wong, O. K. and Fang, G. (2006). Loading of the 3F3/2 antigen onto kinetochores is dependent on the ordered assembly of the spindle checkpoint proteins. *Mol. Biol. Cell* **17**, 4390-4399.

Yamagishi, Y., Sakuno, T., Shimura, M. and Watanabe, Y. (2008). Heterochromatin links to centromeric protection by recruiting shugoshin. *Nature* **455**, 251-255.

Yamaguchi, S., Decottignies, A. and Nurse, P. (2003). Function of Cdc2p-dependent Bub1p phosphorylation and Bub1p kinase activity in the mitotic and meiotic spindle checkpoint. *EMBO J.* **22**, 1075-1087.

A

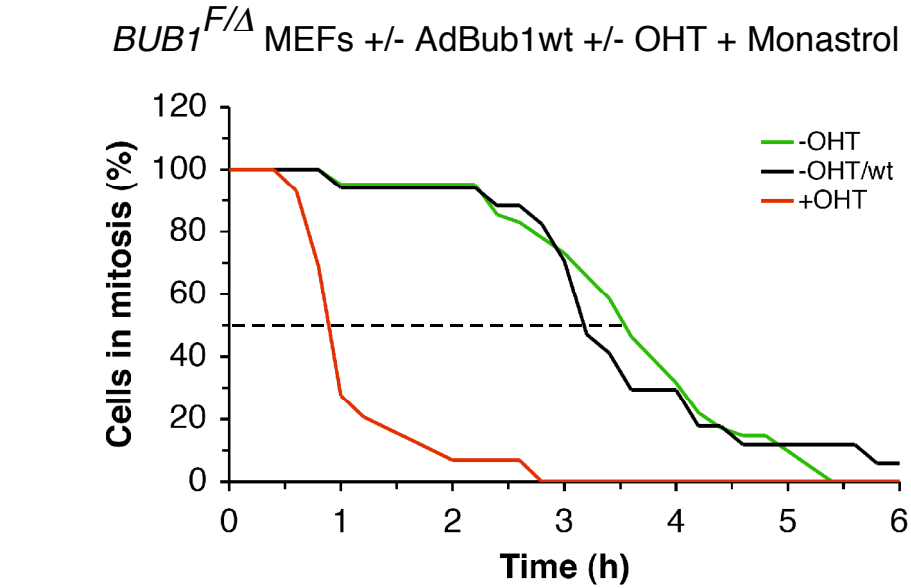
BUB1F/Δ MEFs +/- AdBub1wt +/- OHT + Monastrol
Cells in mitosis (%)
120
100
80
60
40
20
0
0
1
2
3
4
5
6
Time (h)
-OHT
-OHT/wt
+OHT

B

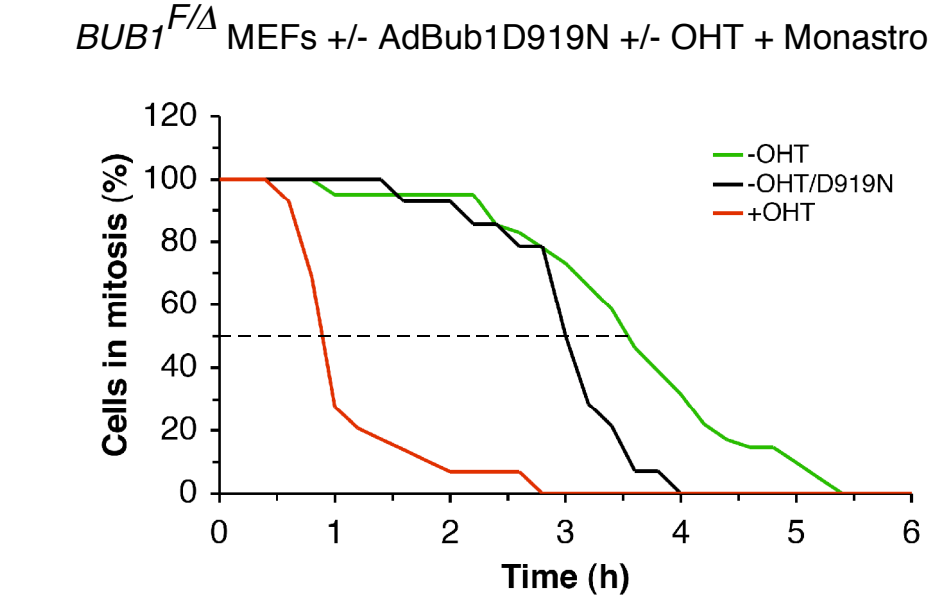
BUB1F/Δ MEFs +/- AdBub1D919N +/- OHT + Monastrol
Cells in mitosis (%)
120
100
80
60
40
20
0
0
1
2
3
4
5
6
Time (h)
-OHT
-OHT/D919N
+OHT

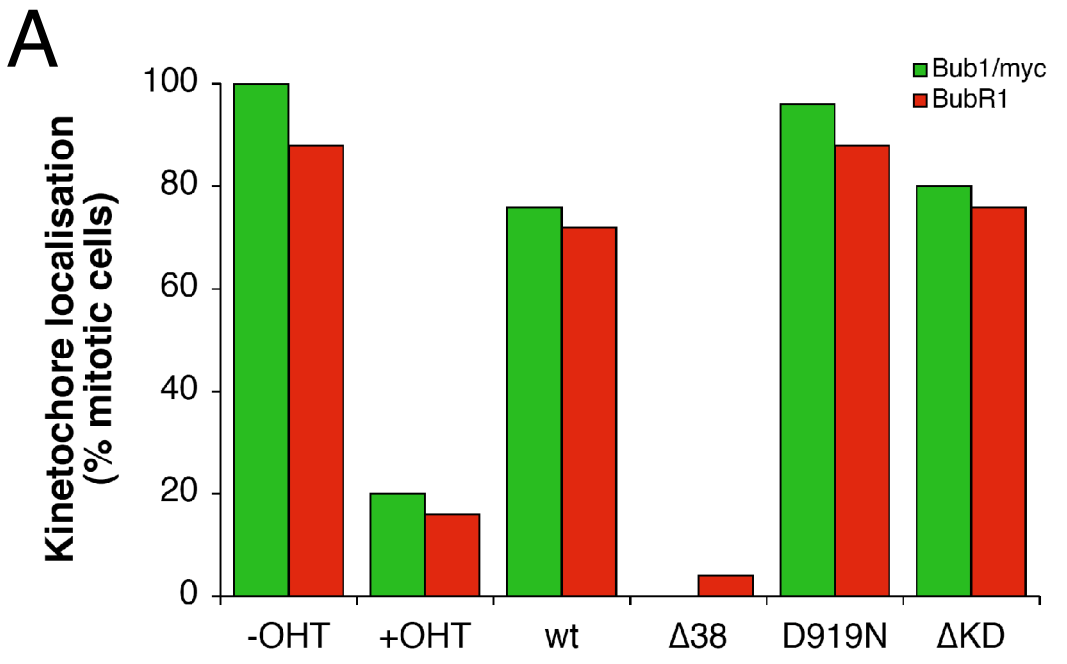
A
Kinetochore localisation
(% mitotic cells)
100
80
60
40
20
0
Bub1/myc
BubR1
-OHT
+OHT
wt
Δ38
D919N
ΔKD

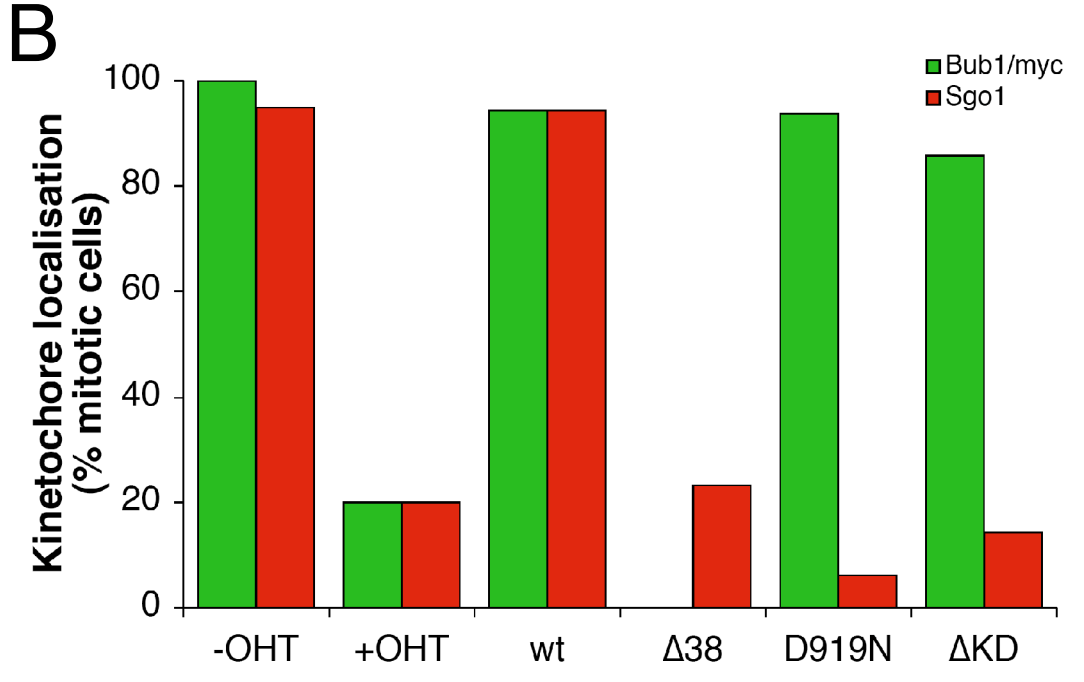
B
Kinetochore localisation
(% mitotic cells)
100
80
60
40
20
0
Bub1/myc
Sgo1
-OHT
+OHT
wt
Δ38
D919N
ΔKD

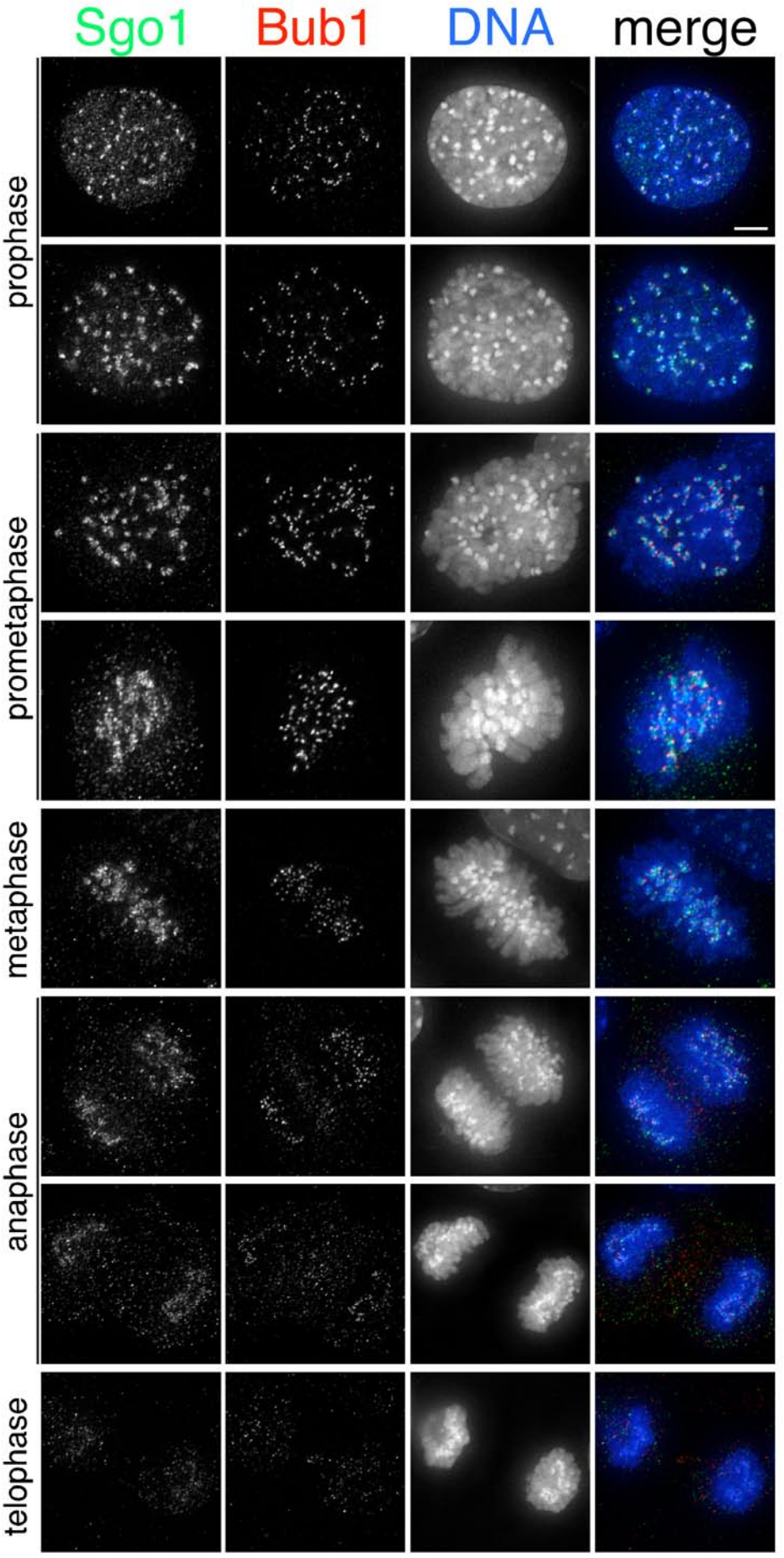
Sgo1
Bub1
DNA
merge
prophase
prometaphase
metaphase
anaphase
telophase

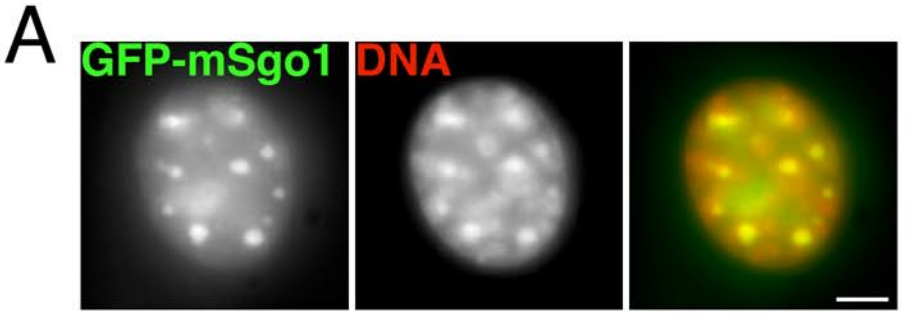
A
GFP-mSgo1
DNA

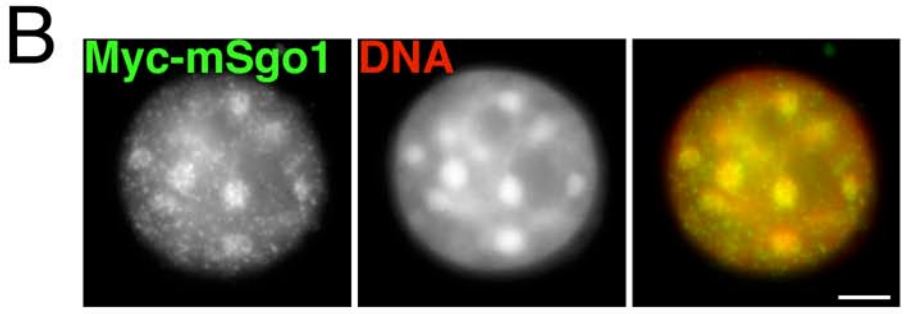
B
Myc-mSgo1
DNA

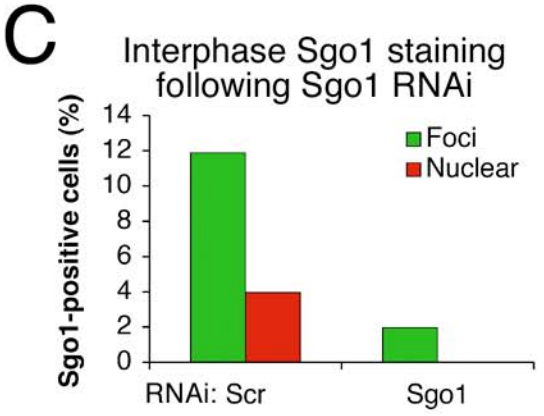
C
Interphase Sgo1 staining following Sgo1 RNAi
Sgo1-positive cells (%)
0
2
4
6
8
10
12
14
Foci
Nuclear
RNAi: Scr
Sgo1

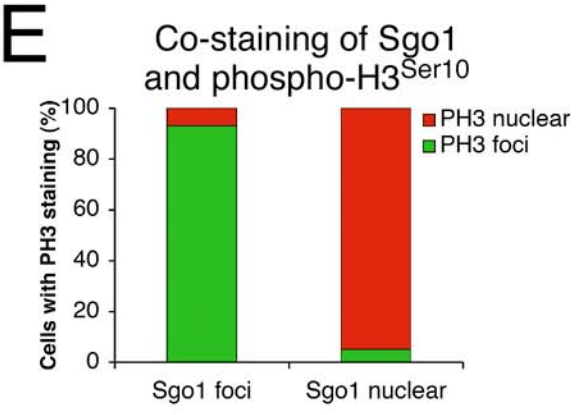
E
Co-staining of Sgo1 and phospho-H3Ser10
Cells with PH3 staining (%)
0
20
40
60
80
100
PH3 nuclear
PH3 foci
Sgo1 foci
Sgo1 nuclear

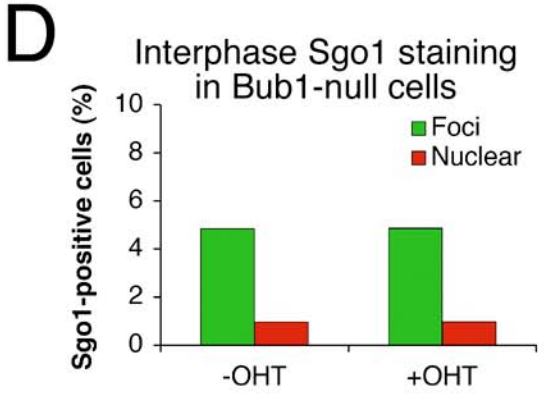
D
Interphase Sgo1 staining in Bub1-null cells
Sgo1-positive cells (%)
0
2
4
6
8
10
Foci
Nuclear
-OHT
+OHT

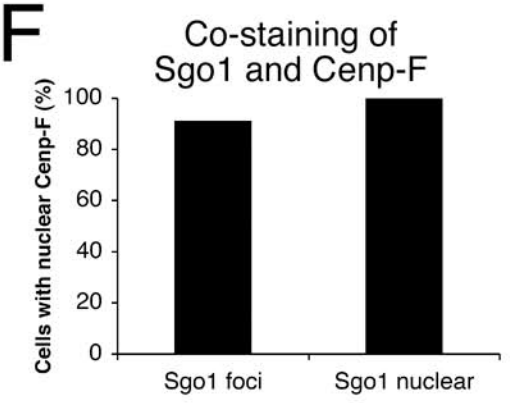
F
Co-staining of Sgo1 and Cenp-F
Cells with nuclear Cenp-F (%)
0
20
40
60
80
100
Sgo1 foci
Sgo1 nuclear

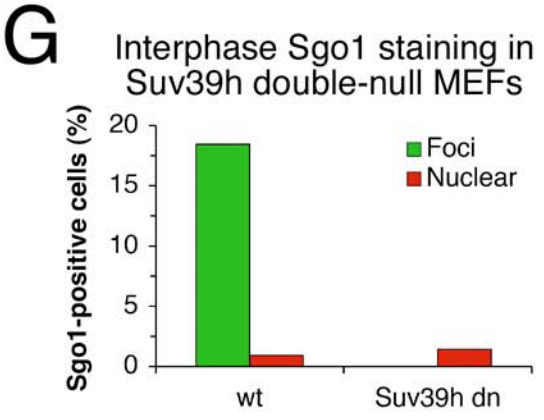
G
Interphase Sgo1 staining in Suv39h double-null MEFs
Sgo1-positive cells (%)
0
5
10
15
20
Foci
Nuclear
wt
Suv39h dn